

An Azide-Insensitive Superoxide Dismutase from a Hyperthermophilic Archaeon, *Sulfolobus solfataricus*¹

Shigeyuki Yamano^{*2} and Tadashi Maruyama[†]

^{*}Marine Biotechnology Institute, Shimizu Laboratories, Shimizu, Shizuoka 424-0037; [†]Marine Biotechnology Institute, Kamaishi Laboratories, Kamaishi, Iwate 026-0001

Received June 2, 1998; accepted October 9, 1998

The superoxide dismutase (SOD) gene of *Sulfolobus solfataricus*, a hyperthermophilic archaeon, was cloned and expressed in *Escherichia coli*, and its gene product was characterized. When the protein was expressed in *E. coli*, it formed a homodimer that contained both Mn and Fe. Metal reconstitution experiments of the SOD with Fe or Mn showed that only the Fe-reconstituted SOD was active. Substitution of Tyr88 to Phe did not affect the metal specificity of the enzyme. The Fe-reconstituted SOD was extremely resistant to thermal denaturation; e.g. 96% of the initial activity was retained after heating at 95°C for 2 h. Fe-reconstituted SOD was not inhibited by azide, but fluoride inhibition was observed. This suggests that some steric hindrance in the substrate funnel of the enzyme prevents the access of N₃⁻ but allows O₂⁻ and F⁻ access to the active site.

Key words: archaea, azide, hyperthermophile, *Sulfolobus solfataricus*, superoxide dismutase.

Superoxide dismutases (SODs) are widely distributed among aerobic organisms in which they catalyze the dismutation of the superoxide anion (O₂⁻) to O₂ and H₂O₂. SODs play an important role in cell protection mechanisms against oxidative damage. These enzymes comprise a family of metalloproteins classified into three main groups according to their metal cofactor: copper and zinc-containing SOD (Cu,Zn-SOD), manganese-containing SOD (Mn-SOD), and iron-containing SOD (Fe-SOD). The latter two groups are assumed to have a common evolutionary origin because of the close similarity in their amino acid sequences and three-dimensional protein structures, whereas Cu,Zn-SODs apparently evolved independently. There is little difference in catalytic activity between Mn-SOD and Fe-SOD. Despite these similarities, metal-reconstitution studies indicate that most Mn- and Fe-SODs show strict metal specificity (1, 2). A few groups of bacteria possess "cambialistic" SODs that are active with either Fe or Mn as a cofactor. It is unknown how the metal specificity of SOD is determined.

Hyperthermophilic bacteria and archaea occupy all the deepest and shortest branches of the phylogenetic tree (3). Therefore, they might retain primitive characteristics close to the common ancestor of all beings on earth. The characterization of hyperthermophilic SODs is interesting from a speculative viewpoint of the evolution of Mn- and Fe-SODs.

Although a few Fe-SODs have been purified from hyperthermophilic archaea, including *Sulfolobus solfataricus* (4) and *S. acidocaldarius* (5), their sensitivities to inhibitors and metal specificities were not well characterized. Here we report the cloning and characterization of a superoxide dismutase from an acidophilic hyperthermophilic archaeon, *Sulfolobus solfataricus*. This SOD is azide-insensitive, and the mechanism of its azide-insensitivity is discussed.

MATERIALS AND METHODS

Strains and Enzymes—*S. solfataricus* DSM 1616 was obtained from Deutsche Sammlung von Mikroorganismen und Zellkulturen GmbH. It was grown in Brock's medium (6) at 75°C with vigorous rotary shaking (180 rpm). Cells in the late exponential growth phase were harvested by centrifugation and washed twice with fresh medium. The cell pellet was frozen at -80°C prior to DNA isolation. *Escherichia coli* Fe-SOD (S5389) and Mn-SOD (S5639) were purified enzymes purchased from Sigma (St. Louis, USA).

Preparation of Genomic DNA—Cells (1 g wet weight) were suspended in 19 ml of lysis buffer containing 50 mM Tris-HCl (pH 8.0), 50 mM EDTA, 0.5% sodium lauryl sarcosinate, and 0.2 mg/ml proteinase K, and incubated at 50°C for 3 h. The lysate was extracted once with phenol and twice with phenol/chloroform. After precipitation with 2 volumes of ethanol, the DNA was dissolved in 3 ml of TE buffer (10 mM Tris-Cl, pH 8.0, 1 mM EDTA). The DNA solution was incubated with 0.025 mg/ml RNase A at 37°C for 1 h and then with 0.05 mg/ml proteinase K and 0.5% SDS at 50°C for 1 h. The solution was extracted twice with phenol/chloroform. After precipitation with 2 volumes of ethanol, the DNA was dissolved in 2 ml of TE buffer.

Amplification of a Part of the SOD Gene by PCR—Two

¹ Nucleotide sequence accession number: AB012620.

² To whom correspondence should be addressed at the present address: Central Laboratory for Key Technology, Kirin Brewery Co., Ltd., 1-13-15 Fukuura, Kanazawa-ku, Yokohama, Kanagawa 236-0004. Phone: +81-045-788-7214, Fax: +81-045-788-4042, E-mail: syamano@kirin.co.jp

PCR primers designed from conserved sequences of reported SODs were synthesized.

SODF3: 5'-GA(TC)GC(GATC)(TC)T(GATC)GA(AG)-CC(GATC)-3'

SODR1: 5'-(GA)TA(AG)(TA)A(GATC)(GC)(CAT)(AG)-TG(TC)TC(CAGT)-3'

The PCR reaction was performed using 1.7 ng/ μ l of genomic DNA as the template with 2 μ M SODF3 and 8 μ M SODR1. The PCR reaction was started with a template denaturation step at 95°C for 4 min followed by 30 repetitions of temperature cycling for amplification. The profile for amplification was 95°C for 0.5 min, 44°C for 0.5 min, and 72°C for 1 min. The PCR-amplified fragment with the expected size (453–477 bp) was ligated to pT7Blue-T (Novagen, Madison, USA) and its sequence was determined.

Construction and Screening of the Cosmid Library—Genomic DNA was partially digested with *Sau*3AI and ligated to SuperCos1 (Stratagene, La Jolla, USA) digested with *Bam*HI. The ligated DNA was packaged *in vitro* and introduced into *E. coli* XL1-Blue MR according to Stratagene's instruction manual. Ampicillin-resistant transformants were obtained at a frequency of 4.5×10^4 per μ g of ligated DNA. This genomic library was screened by colony hybridization using the PCR-amplified fragment as a probe. Labeling of the probe and hybridization were carried out using a DIG DNA labeling and detection kit (Boehringer Mannheim, Mannheim, Germany). The selected plasmid was called pSODSS2.

Expression of the SOD Gene—Two PCR primers were synthesized. SSF3 contained the recognition sequence of *Nde*I upstream of the initiation codon of the ORF. SSR3 contained the recognition sequence of *Bam*HI downstream of the stop codon of the ORF.

SSF3: 5'-GCGCATATGACTCTCCAAATTCAGT-3'

SSR3: 5'-CGCGGATCCAACTATTACTTCGTTAAA-TATTT-3'

After PCR-amplification of the plasmid pSODSS3 containing the SOD gene, the amplified fragment was digested with *Nde*I and *Bam*HI, and then ligated into vector pET11a (Stratagene) which was digested with the same enzymes in order to construct plasmid pSODSS5 for the expression of the *S. solfataricus* SOD gene in *E. coli*. *E. coli* BL21(DE3) was transformed with pSODSS5. The transformant was grown in LB medium at 30 or 37°C up to logarithmic phase, and then 0.2–1.0 mM isopropyl β -D-thiogalactopyranoside (IPTG) was added to the culture to induce the SOD gene. The cells were then grown at 30 or 37°C to stationary phase. For metal-rich cultures, 0.5 mM $MnSO_4$ or $FeSO_4$ was added to the medium.

Purification of the SOD Gene Product—Harvested cells were suspended in 50 mM Tris-HCl (pH 8.0) and sonicated 2 times for 2.5 min on ice with a Sonifier 250 (Branson, Danbury, USA). After incubation at 75°C for 30 min, the lysate was centrifuged at $9,730 \times g$ for 20 min to precipitate denatured *E. coli* proteins. The supernatant was concentrated with Centriprep-10 (Amicon, Beverly, USA) and applied to a Q-Sepharose HP HiLoad 16/10 column (Pharmacia LKB, Uppsala, Sweden) and eluted with a linear NaCl gradient (0–0.6 M) in 50 mM Tris-HCl (pH 8.0). Fractions containing SOD activity were concentrated with Centriprep-10 (Amicon). Protein concentration was measured by the method of Bradford (7) using bovine serum

albumin as a standard. The enzymes at each step were analyzed by SDS-PAGE in 18% gels.

For molecular mass estimation, SOD was applied to a Superose 12 HR 10/30 column (Pharmacia) equilibrated with 50 mM Sodium phosphate (pH 7.0) + 150 mM NaCl buffer at a flow rate of 0.4 ml/min. The elution profile was monitored by absorbance at 280 nm.

Assays for Superoxide Dismutase Activity—Enzyme activity was assayed at 25°C by the xanthine oxidase-cytochrome c method (8). One unit is defined as the amount of enzyme that causes 50% inhibition of cytochrome c reduction. To determine the effects of inhibitors, activity was measured in reaction mixtures containing inhibitors. In H_2O_2 inactivation experiments, SOD (0.25 mg/ml) was incubated with 0.24 mM H_2O_2 in 50 mM potassium phosphate (pH 7.8) at 25°C. At intervals, aliquots were withdrawn, treated with catalase (1.0 U/ μ l), and then the residual activity was assayed. In thermal inactivation experiments, reaction mixtures containing 1 mg/ml SOD in 20 mM potassium phosphate (pH 7.0) were incubated at 90–105°C. Aliquots were removed at intervals, chilled on ice, and the residual activity was measured.

Reconstitution of SOD—The purified SOD (3.0 mg) was incubated in 3 ml denaturation buffer (50 mM acetate buffer, pH 3.8, containing 6 M guanidine hydrochloride, and 10 mM EDTA) for 16 h at 50°C. The solution was gel-filtered through a Sephadex G-25 column (Pharmacia) equilibrated with denaturation buffer to obtain the apoprotein. For the preparation of the Mn-reconstituted enzyme, the apoprotein was dialyzed against 50 mM acetate buffer, pH 3.8, containing 6 M guanidine hydrochloride and 10 mM $MnSO_4$ for 4 h at room temperature, then against 50 mM Tris-HCl buffer, pH 7.5, containing 6 M guanidine hydrochloride and 10 mM $MnSO_4$ for 4 h at room temperature. The guanidine hydrochloride was removed by dialysis against 50 mM Tris-HCl buffer, pH 7.5, containing 1 mM $MnSO_4$ for 4 h at room temperature, then against 50 mM Tris-HCl buffer, pH 7.5, containing 0.5 mM EDTA for 12 h at room temperature. The Mn-reconstituted enzyme was obtained after gel filtration through a Sephadex G-25 column (Pharmacia) equilibrated with 50 mM Tris-HCl buffer, pH 7.5. The Fe-reconstituted enzyme was prepared by the same procedures using $FeSO_4$ instead of $MnSO_4$.

Metal Analysis—The metal content of the purified SOD was determined with an Inductively Coupled Plasma Emission Spectrometer (ICPS-1000 IV, Shimadzu, Kyoto).

Mass Spectrometry Analysis—MALDI-TOF mass spectra were obtained in the positive ion mode using a Voyager Elite time-of-flight mass spectrometer (PerSeptive Biosystems, Framingham, USA). The matrix was prepared by dissolving sinapinic acid (10 mg/ml) in 33.3% acetonitrile and 0.0667% trifluoroacetic acid (TFA). Purified SOD (0.5 μ l) dissolved in 0.005% TFA was mixed with 4.5 μ l of the matrix to give a final concentration of 7.2 pmol/ μ l. The mixed sample (0.5 μ l) was applied to the target plate and allowed to evaporate. The spectra were obtained using a linear-mode measurement. The ions generated by laser (337 nm) irradiation were accelerated to 20 kV and passed through a 2.0 m flight tube to the detector. ACTH(7-38) fragment (+1): M_r 3,660.17 and myoglobin (+1): M_r 16,952.56 were used for calibration.

Amino Acid Sequence Determination—The N-terminal amino acid sequence of the purified SOD was determined by

a Shimadzu PSQ-2 protein sequencer (Shimadzu).

Site Directed Mutagenesis—Mutagenesis of the *S. solfataricus* SOD gene was carried out according to the overlap extension method (9). Two PCR primers were synthesized as described below. SSR1 consisted of the native anti-sense sequence while SS-Y88F consisted of a mutation (AT→TC) and the other native sense sequence.

SSR1: 5'-TATGATTTTGGGAAGTGATTTTC-3'

SS-Y88F: 5'-GGACACAAGTTACACGCCTTGTCTG-GGAAAATATG-3'

The first step consisted of two simultaneous PCR reactions, the first with primers SSF3 and SSR1 and the second with primers SS-Y88F and SSR3. These PCR reactions containing 2 ng/μl pSODSS5 as the template were started with a template denaturation step at 95°C for 3 min followed by 25 repetitions of temperature cycling for amplification. The profile for amplification was 95°C for 0.5 min, 52°C for 0.5 min, and 72°C for 1 min. The amplified products were purified by ultrafiltration (Suprec 02; Takara Shuzo). Each purified fragment (60 ng) was mixed and subjected to 25 cycles of PCR under the same conditions as described above with primers SSF3 and SSR3. After purification, the amplified product was digested with *Nde*I and *Bam*HI and then ligated to the vector pET11a (Stratagene), which was then digested with the same enzymes in order to construct plasmid pSSF88 for the expression of the Tyr88→Phe mutant SOD (Y88F mutant) in *E. coli*. Mutagenesis was confirmed by DNA sequencing. *E. coli* BL21(DE3) was transformed with pSSF88. The expression, purification, and reconstitution of Y88F mutant were done in the same way as in the case of rSOD.

RESULTS

Cloning and Structure of the SOD Gene—Although the sequences of 20 PCR-amplified fragments were determined, only one sequence homologous to SOD genes was detected. This DNA fragment was considered to be part of the SOD gene because of its similarity to known Fe- and Mn-SOD genes. The genomic library was screened with this fragment as a probe. Among several positive clones, one was selected for further research and its plasmid was designated pSODSS2. Plasmid pSODSS2 was partially digested with *Sau*3AI and ligated to pUC18. The resulting plasmids were screened by colony hybridization using the same probe. Plasmid pSODSS3 containing a 4.6 kb genomic fragment was obtained and its nucleotide sequence was determined. The open reading frame obtained was thought to be the *S. solfataricus* SOD (SS-SOD) gene due to its similarity to other known Fe- and Mn-SOD genes. The upstream region of the SS-SOD gene is shown in Fig. 1. The amino acid sequence deduced from the nucleotide sequence of the cloned SOD gene agreed perfectly with that of the SOD protein purified from *S. solfataricus* cells (native SS-SOD; nSS-SOD), except for the N-terminal Met (4). The latter had no Met at its N-terminus.

Fig. 1. The upstream region of the *S. solfataricus* SOD gene. BoxA and boxB sequences are indicated by underlines and dotted lines, respectively. Nucleotide sequence accession number: AB012620.

```

1  ATTAATAACTGCAACTATTACTCTATTTATATATTCATATACAATATCACTATTTGGCTC 60
61  CATGTTCTTTATAAACATACTTAGAATAATATATCTCTCAAGATATATATGGTTTACT 120
121 AGCTTTAGTAAGTTAAAGATATAAACGGTCTTCATATCTATACCTATGACTCTCCAAAT 180
      M T L Q I

```

A pair of conserved sequences has been repeatedly found in archaeal promoters (10). One is a highly conserved TATA-box like boxA, TTTA(A/T)A. The other is a weakly conserved boxB, (A/T)TG(A/C) located at the transcription start site. The distance between boxA and boxB is 22 to 27 bp. Two sets of promoter-like elements were found upstream of the ORF in the SS-SOD gene. The first pair of putative boxA and boxB sequences was found 141 and 107 bp upstream of the initiation codon, respectively. The second putative boxA sequence was found 27 bp upstream of the initiation codon with a slight variation, TATAAA. The corresponding boxB sequence overlapped the initiation codon. The latter pair may be the major promoter element of the SS-SOD gene because transcription starts near initiation codons in other archaeal SOD genes (11, 12).

Expression and Purification of *S. solfataricus* Recombinant SOD—The transformant *E. coli* cells harboring the expression plasmid pSODSS5 were sonicated and heated to remove *E. coli* proteins containing endogenous SOD. The concentrated supernatant was applied to a Q-Sepharose column, and *S. solfataricus* recombinant SOD (rSS-SOD) was eluted in the void volume. As shown in Fig. 2, the rSS-SOD was purified to homogeneity. The apparent molecular weight of the monomer was estimated to be 25,200 from SDS-PAGE, which agrees approximately with the value, 24,243.08, calculated from the deduced amino acid sequence. This value also agrees with that of nSS-SOD. The N-terminal amino acid sequence of rSS-SOD showed it to be a mixture of a peptide starting with an initial Met and a truncated peptide without the initial Met. The truncated SOD, which appears to be identical to nSS-SOD, occupies approximately 90% of rSS-SOD. The molecular weights estimated from the nucleotide sequences agreed well with the values, 24,233.5 and 24,110.6, ob-

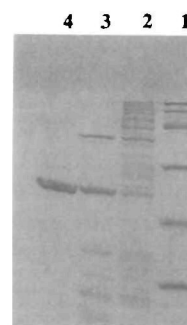


Fig. 2. SDS-PAGE of the purification step products. Aliquots from the various purification steps were analyzed by SDS-PAGE in an 18% gel. Each lane contains 5 μg of protein. The gel was stained with Coomassie Brilliant Blue. Lane 1, protein size markers (from top to bottom): 97.4, 66.2, 45.0, 31.0, 21.5, and 14.4 kDa; lane 2, cell lysate supernatant after sonication; lane 3, cell lysate supernatant after heat treatment (for 30 min at 75°C); lane 4, after Q-Sepharose column chromatography.

tained by MALDI-TOF mass spectrometry, thus suggesting that the SS-SOD is not modified in *E. coli*. The apparent molecular weight of the whole enzyme estimated by gel filtration indicates that rSS-SOD, like nSS-SOD, forms a homodimer in *E. coli* cells.

Metal Cofactor—It has been reported that nSS-SOD does not contain Mn, but rather 0.7 atom of Fe per subunit (4). However, rSS-SOD always contains both Mn and Fe, although its metal content varies according to the conditions of gene expression and culture. The activity appears to depend on the Fe content but not the Mn content (Fig. 3). To determine the metal-specificity of rSS-SOD, metal-reconstitution experiments were carried out. As shown in Table I, Fe-reconstituted rSS-SOD contains 0.88 atom of iron per subunit and a specific activity of 481 U/mg protein. Mn-reconstituted rSS-SOD contains 0.80 atom of manganese per subunit but virtually no activity (1.2 U/mg protein). Therefore, we conclude that rSS-SOD is active only with Fe as a cofactor, while the incorporation of Mn is almost equivalent to that of Fe. The specific activity of Fe-reconstituted rSS-SOD is approximately 13–16% of eubacterial Fe-SODs at 25°C (13). This temperature is probably lower than the optimum temperature because the optimum growth temperature of *S. solfataricus* is 87°C (14). Because xanthine oxidase in the assay mixture for SOD is not thermostable, the activity was measured at 25°C (4, 5, 18, 20, 21).

Thermal Inactivation—*S. solfataricus* grows between 50 and 87°C with an optimum growing temperature of 87°C, but it neither grows nor survives at 90°C (14). At 85–90°C, which is close to the non-permissive temperature for growth, no loss of activity of the Fe-reconstituted rSS-SOD was observed even after 2 h incubation (Fig. 4). At 95–105°C, rSS-SOD was inactivated according to first order kinetics. Half-lives were extrapolated to 33 h at 95°C, 8.7 h

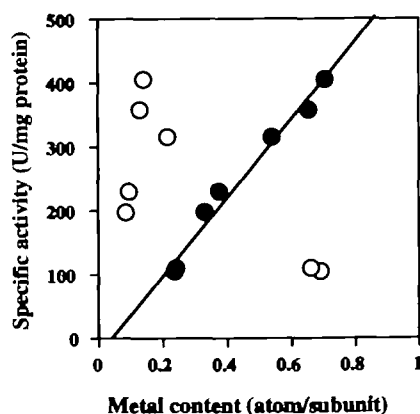


Fig. 3. Activity vs. metal content of *S. solfataricus* SODs produced in *E. coli* cells. Open circles, Mn; closed circles, Fe.

TABLE I. Activity and metal content of metal-reconstituted rSOD.

Enzyme	Metal content (atom/subunit)		Specific activity (U/mg protein)
	Fe	Mn	
Fe-reconstituted SOD	0.88 ± 0.02	<0.01	481 ± 10
Mn-reconstituted SOD	<0.01	0.80 ± 0.02	1.2 ± 0.04

Data are averages of two or three independent experiments.

at 100°C, and 1.5 h at 105°C. The Fe-SOD from the hyperthermophilic bacterium *Aquifex pyrophilus* loses about 20% of its initial activity after 2 h incubation at 95°C (15). This shows the extreme thermostability of Fe-reconstituted rSS-SOD.

Effect of Inhibitors and Hydrogen Peroxide on SOD Activity—Sodium azide competitively inhibits all types of SODs. The concentrations of sodium azide that cause 50% inhibition of *E. coli* Fe-SOD and *E. coli* Mn-SOD are 4 and 22 mM, respectively, agreeing approximately with the values previously reported (16) (Fig. 5). However, up to 100 mM sodium azide did not inhibit the Fe-reconstituted rSS-SOD. rSS-SOD is thus anomalously resistant to sodium azide inhibition. The absorption spectra of Fe-reconstituted rSS-SOD with and without sodium azide were compared to those of *E. coli* Fe-SOD. In the presence of sodium azide, new absorption bands appeared near 420 nm in *E. coli* Fe-SOD, as reported previously (13). In contrast, no change in the spectrum was observed for Fe-reconstituted rSS-SOD. This indicates that azide does not bind to Fe at the active site of rSS-SOD. Sodium fluoride, another inhibitor that binds to metal at the active site, inhibits both

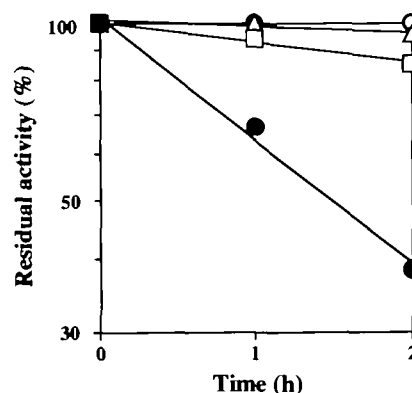


Fig. 4. Thermal inactivation of reconstituted *S. solfataricus* Fe-SOD. Residual activity is represented in logarithmic scale. Open circles, 90°C; open triangles, 95°C; open squares, 100°C; closed circles, 105°C.

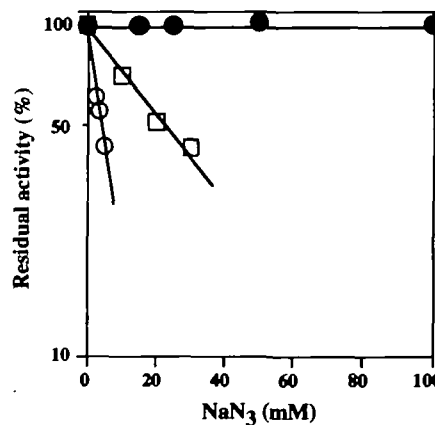


Fig. 5. Effect of sodium azide on reconstituted *S. solfataricus* Fe-SOD. Residual activity is represented in logarithmic scale. Closed circles, *S. solfataricus* SOD; open circles, *E. coli* Fe-SOD; open squares, *E. coli* Mn-SOD.

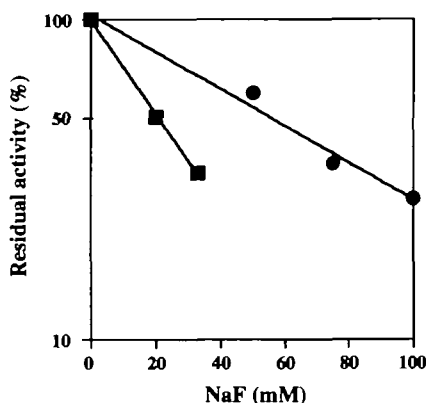


Fig. 6. Inactivation of SODs by sodium fluoride. Residual activity is represented in logarithmic scale. Closed circles, Fe-reconstituted *S. solfataricus* SOD; closed squares, *E. coli* Fe-SOD.

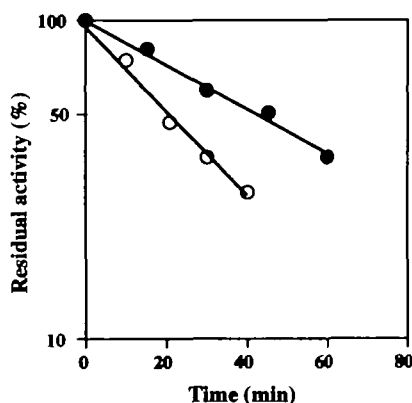


Fig. 7. Inactivation of reconstituted *S. solfataricus* Fe-SOD by hydrogen peroxide. Residual activity is represented in logarithmic scale. Closed circles, *S. solfataricus* SOD; open circles, *E. coli* Fe-SOD.

E. coli Fe-SOD and the Fe-reconstituted rSS-SOD (Fig. 6). The concentrations of sodium fluoride that cause 50% inhibition of *E. coli* Fe-SOD and the Fe-reconstituted rSOD are 20 mM and 53 mM, respectively.

The criterion that distinguishes Fe-SOD from Mn-SOD is inactivation by hydrogen peroxide, which inactivates only Fe-SOD (17). The Fe-reconstituted rSS-SOD is inactivated by hydrogen peroxide, but its sensitivity is lower than that of *E. coli* Fe-SOD as shown in Fig. 7. The inactivation of Fe-reconstituted rSS-SOD fits first order kinetics.

Characterization of the Y88F Mutant—While Fe- and Mn-SODs have been shown to have similar primary and three-dimensional structures, it has been reported that some amino acid residues differ between Mn- and Fe-SODs (18, 19). Tyr88 of SS-SOD is presumably specific to Fe-SODs. In Mn-SODs, this residue is commonly Phe. In order to test the above hypothesis, we replaced Tyr88 in SS-SOD with Phe to make the mutant Y88F. The apparent molecular weight of the Y88F mutant found to agree with that of wild type rSOD on SDS-PAGE. The metal contents and activities of metal-reconstituted Y88F mutants are shown in Table II. The Y88F mutant is actually active only

TABLE II. Activity and metal content of metal-reconstituted Y88F mutant SOD.

Enzyme	Metal content (atom/subunit)		Specific activity (U/mg protein)
	Fe	Mn	
Fe-reconstituted SOD	0.82±0.03	0.02	755±20
Mn-reconstituted SOD	0.03	0.85±0.03	4.3±0.3

Data are averages of two independent experiments.

with Fe as a cofactor although the incorporation of Mn is almost equivalent to that of Fe. Thus, the metal specificity of the Y88F mutant is similar to that of rSOD. However, the specific activity per metal atom increased 1.7 times.

DISCUSSION

Fe-SODs from the thermophilic archaea *M. thermoautotrophicum* (20) and *M. bryantii* (21) are known to be relatively azide-resistant. The former is 32% inhibited by 10 mM, and the latter is 50% inhibited by 15 mM azide. Although nSS-SOD was described as an azide-insensitive SOD, no data were presented in the previous report (4). The inhibition of *S. acidocaldarius* Fe-SOD by azide has not been reported (5). Usually, Fe-SOD is more sensitive to sodium azide than Mn-SOD is (16). Therefore, the azide-insensitivity of rSS-SOD is unique. This is not an artificial characteristic in a recombinant SOD produced in *E. coli* because the *M. thermoautotrophicum* SOD produced in *E. coli* is azide-sensitive as described above (20). On the other hand, fluoride inhibits the Fe-reconstituted rSS-SOD. In *E. coli* Fe-SOD, the ligand, substrate or inhibitor, approaches the metal ion at the active site through the substrate funnel formed at the interface of two monomers in the homodimer of SOD (22). rSS-SOD forms a homodimer and has four residues (His-39, Tyr-42, His-85, Trp-89) postulated to be in the substrate funnel. Therefore, it is likely that the substrate funnel is also formed in rSS-SOD. rSS-SOD may have some steric hindrance in the substrate funnel that allows access to O_2^- and F^- to the active site but prevents access by N_3^- because the molecular size of N_3^- is larger than O_2^- and F^- . This hypothesis is supported by the absorption spectra which suggest that azide can hardly bind to Fe at the active site.

Amino acid analysis of native and hydrogen peroxide-treated Fe-SOD from *Pseudomonas ovalis* (23) and *E. coli* (24) has shown that hydrogen peroxide inactivation is accompanied by the specific loss of Trp residues, leaving the other amino acid residues substantially unchanged. Beyer and Fridovich (24) have proposed that iron in the active center may induce the disruption of Trp close to the iron, possibly by a Fenton-type reaction (25). Multiple alignment of the known amino acid sequences of Fe- and Mn-SODs shows that most SODs that are resistant to hydrogen peroxide lack a Trp residue at position 83 (numbering based on the *S. solfataricus* sequence), which is close to the metal-binding His-85 (26). The corresponding Trp residue is not found in rSS-SOD (Fig. 8). The absence of this Trp residue may be why rSS-SOD has a lower H_2O_2 sensitivity.

Large networks of ion-pairs are found in hyperthermophilic glutamate dehydrogenases (27) and indol-3-glycerol-phosphate synthases (28). Ion-pair networks are thought to

contribute to the hyperthermostability of *A. pyrophilus* SOD because it contains many charged residues (24.9%; 15). While the charged residue content of rSS-SOD (19.4%) is comparable to that of mesophiles and less than that of *A. pyrophilus* SOD, its thermostability is slightly higher than that of *A. pyrophilus* SOD. Therefore, some other unknown factor may contribute to the hyperthermostability of rSS-SOD.

Parker and Blake found that five amino acid residues differ among six Mn- and three Fe-SODs of bacterial and eukaryotic origin (18). These residues are shown in Fig. 8

with the positions numbered to correspond to the sequence of SS-SOD. In Mn-SODs, residues at positions 80, 81, 88, 156, and 157 are G, G, F, Q, and D, respectively. In Fe-SODs, the corresponding residues are A, Q, Y, A, and G, respectively. Yamakura suggested that the most probable among these residues to determine the metal specificity of five Mn- and three Fe-SODs are those at positions 81, 88, and 156 (19). However, in archaeal SODs, the residues at 80, 81, 156, and 157 do not seem to obey the rule, but Tyr at 88 appears possible. Tyr 88 is found in all Fe-SODs except that in *M. thermoautotrophicum* Fe-SOD. Because

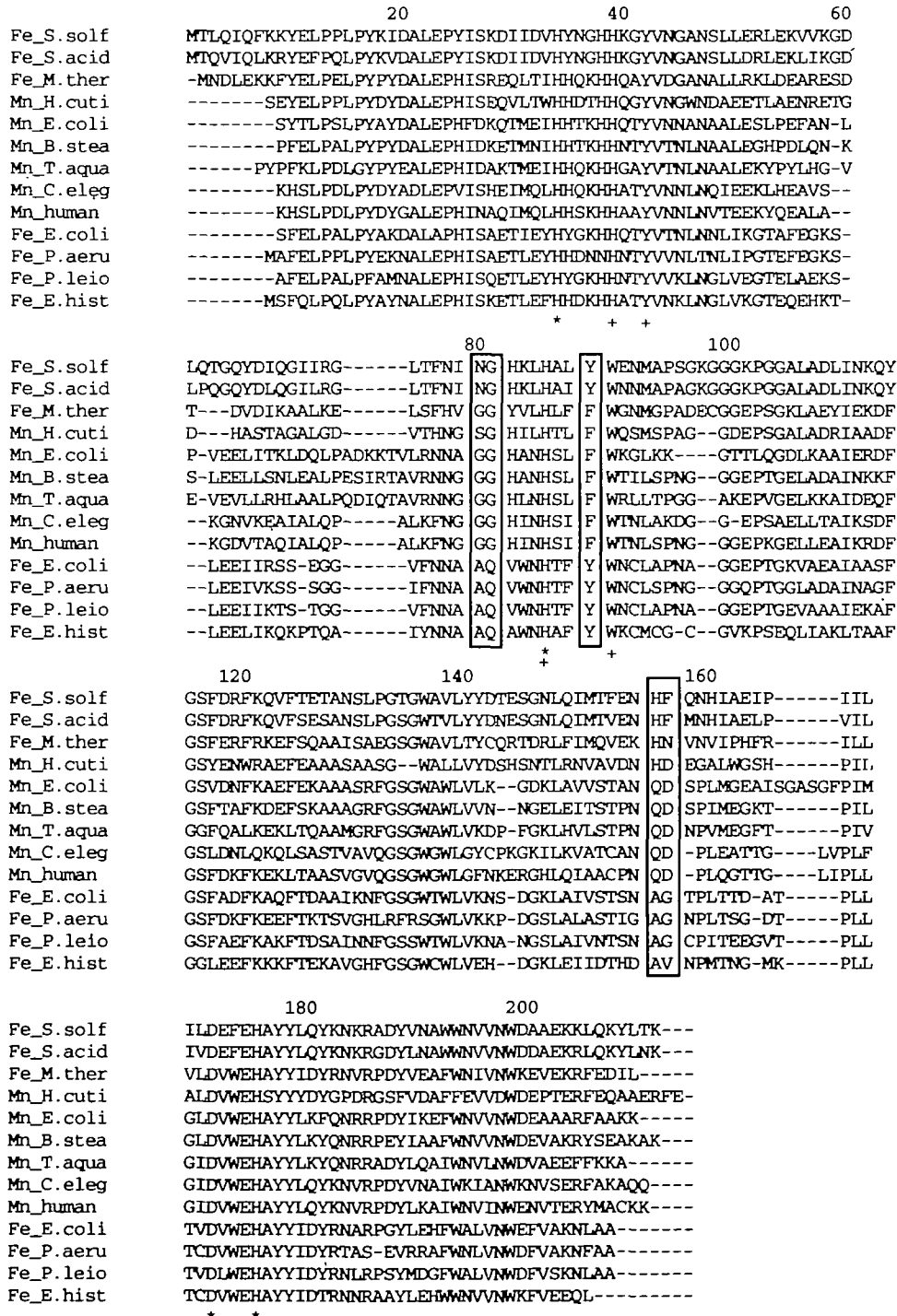


Fig. 8. Aligned amino acid sequences of Mn- and Fe-SODs. Sequences were obtained from the SWISS-PLOT and DDBJ databases and aligned using the program CLUSTAL W (37). Positions are numbered to correspond to the sequence of SS-SOD. Residues postulated to be metal-binding and part of the substrate funnel are indicated by asterisks (*) and +, respectively. Residues that may distinguish between Mn-, and Fe-SODs are indicated by boxed letters. The upper four sequences are those of archaeal SODs. Abbreviations: Mn-, Mn-SOD; Fe-, Fe-SOD; E.coli, *E. coli*; B.stea, *Bacillus stearothermophilus*; T.aqua, *Thermus aquaticus*; C.eleg, *Caenorhabditis elegans*; human, human liver; P.aeru, *Pseudomonas aeruginosa*; P.leio, *Photobacterium leiognathi*; E.hist, *Entamoeba histolytica*; S.solf, *S. solfataricus*; S.acid, *S. acidocaldarius*; M.ther, *Methanobacterium thermoautotrophicum*; H.cuti, *Halobacterium cutirubrum*.

the Y88F mutant is active only when it binds Fe, the importance of F or Y at residue no. 88 for metal specificity is not clear. The residues responsible for metal-binding in archaeal SODs may differ from those in bacterial SODs.

Generally, aerobes and facultative anaerobes contain Mn-SOD and/or Fe-SOD while anaerobes and microaerobes possess Fe-SOD (29). While anaerobically grown *Bacteroides fragilis* cells contain only Fe-SOD, oxygen-stressed cells use the same apoenzyme to produce Mn-SOD (30, 31). *E. coli* cells contain both Fe-SOD and Mn-SOD. While Fe-SOD is synthesized in anaerobically and aerobically grown *E. coli* cells, the synthesis of Mn-SOD is induced by exposure to oxygen or O₂⁻ (32, 33). It is likely that microorganisms prefer Mn-SOD to Fe-SOD in aerobic environments. Iron usually exists in redox states of Fe²⁺ or Fe³⁺. Aqueous Fe²⁺ is easily oxidized to Fe³⁺ at biological pH under aerobic conditions, and Fe³⁺ reacts with H₂O to form insoluble ferric hydroxide. Iron is often a growth-limiting nutrient in aerobic environments because of the insolubility of Fe³⁺. In contrast, manganese can be easily incorporated into SOD in aerobic environments because it is soluble. Iron is only soluble in water as Fe²⁺ under anaerobic or acidic conditions. During the Archean era, the oceans may have been depleted of oxygen allowing huge amounts of aqueous Fe²⁺ to exist (34, 35). In such an Fe-rich environment, anaerobic organisms could have acquired prototypes for Fe-containing enzymes, including Fe-SOD. In the late Archean era, oxygenic photosynthetic organisms such as cyanobacteria appeared and began to release oxygen that likely caused a decrease in aqueous iron and enforced further oxidative stress on anaerobic organisms. During the late Archean and early Proterozoic eras, environmental changes including a decrease in aqueous iron and an increase in oxidative stress might have promoted the evolution of Mn-SODs and cambialistic SODs from Fe-SODs, and also incorporation mechanisms for insoluble Fe³⁺ such as siderophores (36). On the other hand, the oxidation of Fe²⁺ to Fe³⁺ and the reaction of Fe³⁺ with H₂O to form ferric hydroxide are suppressed under acidic conditions. *Sulfolobus* spp. inhabit sulfur-rich acidic hot springs (6) where both Fe²⁺ and Fe³⁺ are soluble. Because soluble iron is available, *S. solfataricus* produce Fe-SOD easily in an aerobic environment. This may be one reason why *S. solfataricus* possess Fe-SOD.

We thank Dr. Y. Shizuri of Marine Biotechnology Institute for helpful suggestions. We thank Mr. M. Fukuda of Japan PerSeptive Co. Ltd., for MALDI-TOF Mass Spectrography.

REFERENCES

- Kirby, T.W., Blum, J., Kahane, I., and Fridovich, I. (1980) Distinguishing between Mn-containing and Fe-containing superoxide dismutase in crude extracts of cells. *Arch. Biochem. Biophys.* **201**, 551-555
- Touati, D. (1992) Regulation and protective role of the microbial superoxide dismutases in *Molecular Biology of Free Radical Scavenging Systems* (Scandalios, J.G., ed.) pp. 231-261, Cold Spring Harbor Laboratory Press, New York
- Stetter, K.O. (1994) The lesson of Archaeobacteria in *Early Life on Earth* (Bengtson, S., ed.) pp. 143-151, Columbia University Press, New York
- Russo, A.D., Rullo, R., Nitti, G., Masullo, M., and Bocchini, V. (1997) Iron superoxide dismutase from the archaeon *Sulfolobus solfataricus*: average hydrophobicity and amino acid weight are involved in the adaptation of proteins to extreme environments. *Biochim. Biophys. Acta* **1343**, 23-30
- Kardinahl, S., Schmidt, C.L., Petersen, A., and Schäfer, G. (1996) Isolation, characterization and crystallization of an iron-superoxide dismutase from the crenarchaeon *Sulfolobus acidocaldarius*. *FEMS Microbiol. Lett.* **138**, 65-70
- Brock, T.D., Brock, K.M., Bellay, R.T., and Weiss, R.L. (1972) *Sulfolobus*: a new genus of sulfur-oxidizing bacteria living at low pH and high temperature. *Arch. Microbiol.* **84**, 54-68
- Bradford, M.M. (1976) A rapid and sensitive method for the quantitation of microgram quantities of protein utilizing the principle of protein-dye binding. *Anal. Biochem.* **72**, 248-254
- McCord, J.M. and Fridovich, I. (1969) Superoxide dismutase: an enzymatic function for erythrocyte hemocypre (hemocypre). *J. Biol. Chem.* **244**, 6049-6055
- Mikaelian, I. and Sergeant, A. (1992) A general and fast method to generate multiple site directed mutations. *Nucleic Acids Res.* **20**, 376
- Zillig, W., Palm, P., Reiter, W.D., Gropp, F., Pühler, G., and Klenk, H.P. (1988) Comparative evaluation of gene expression in archaeobacteria. *Eur. J. Biochem.* **173**, 473-482
- May, B.P. and Dennis, P.P. (1989) Evolution and regulation of the gene encoding superoxide dismutase from the archaeobacterium *Halobacterium cutirubrum*. *J. Biol. Chem.* **264**, 12253-12258
- Klenk, H.P., Schleper, C., Schwass, V., and Brudler, R. (1993) Nucleotide sequence, transcription and phylogeny of the gene encoding the superoxide dismutase of *Sulfolobus acidocaldarius*. *Biochim. Biophys. Acta* **1174**, 95-98
- Slykhov, T.O. and Fee, J.A. (1976) Physical and chemical studies on bacterial superoxide dismutases. *J. Biol. Chem.* **251**, 5472-5477
- Zillig, W., Stetter, K.O., Wunderl, S., Schulz, W., Priess, H., and Scholz, I. (1980) The *Sulfolobus*-*Caldariella* Group: Taxonomy on the basis of the structure of DNA-dependent RNA polymerases. *Arch. Microbiol.* **125**, 259-269
- Lim, J.-H., Yu, Y.-G., Choi, I.-G., Ryu, J.-R., Ahn, B.-Y., Kim, S.-H., and Han, Y.-S. (1997) Cloning and expression of superoxide dismutase from *Aquifex pyrophilus*, a hyperthermophilic bacterium. *FEBS Lett.* **406**, 142-146
- Misra, H.P. and Fridovich, I. (1978) Inhibition of superoxide dismutase by azide. *Arch. Biochem. Biophys.* **189**, 317-322
- Asada, K., Yoshikawa, K., Takahashi, M., Maeda, Y., and Enmanji, K. (1975) Superoxide dismutases from a blue-green alga, *Plectonema boryanum*. *J. Biol. Chem.* **250**, 2801-2807
- Parker, M.W. and Blake, C.C.F. (1988) Iron- and manganese-containing superoxide dismutase can be distinguished by analysis of their primary structures. *FEBS Lett.* **229**, 377-382
- Yamakura, F. (1995) Dependence of the activity of manganese enzymes on manganese: a study on manganese superoxide dismutase. *Kagaku Sosetsu* **24**, 124-131
- Takao, M., Yasui, A., and Oikawa, A. (1991) Unique characteristics of superoxide dismutase of a strictly anaerobic archaeobacterium *Methanobacterium thermoautotrophicum*. *J. Biol. Chem.* **266**, 14151-14154
- Kirby, T.W., Lancaster, J.R., and Fridovich, I. (1981) Isolation and characterization of the iron-containing superoxide dismutase *Methanobacterium bryantii*. *Arch. Biochem. Biophys.* **210**, 140-148
- Lau, M.S., Dixon, M.M., Pattridge, K.A., Stallings, W.C., Fee, J.A., and Ludwig, M.L. (1995) Structure-function in *Escherichia coli* iron superoxide dismutase: Comparisons with the manganese enzyme from *Thermus thermophilus*. *Biochemistry* **34**, 1646-1660
- Yamakura, F. (1984) Destruction of tryptophan residues by hydrogen peroxide in iron-superoxide dismutase. *Biochem. Biophys. Res. Commun.* **122**, 635-641
- Beyer, W.F. and Fridovich, I. (1987) Effect of hydrogen peroxide on the iron-containing superoxide dismutase of *Escherichia coli*. *Biochemistry* **26**, 1251-1257
- Meier, B., Sehn, A.P., Michel, C., and Saran, M. (1994) Reaction of hydrogen peroxide with superoxide dismutase from *Propioni-*

- bacterium shermanii*—an enzyme which is equally active with iron or manganese—are independent of the prosthetic metal. *Arch. Biochem. Biophys.* **313**, 296-303
26. Gabbianelli, R., Battistoni, A., Capo, C., Polticelli, F., Rotilio, G., Meier, B., and Desideri, A. (1997) Effect of Val 73→Trp mutation on the reaction of "cambialistic" superoxide dismutase from *Propionibacterium shermanii* with hydrogen peroxide. *Arch. Biochem. Biophys.* **345**, 156-159
 27. Yip, K.S.P., Stillman, T.J., Britton, K.L., Artymiuk, P.J., Baker, P.J., Sedelnikova, S.E., Engel, P.C., Pasquo, A., Chiaraluce, R., Consalvi, V., Scandurra, R., and Rice, D.W. (1995) The structure of *Pyrococcus furiosus* glutamate dehydrogenase reveals a key role for ion-pair networks in maintaining enzyme stability at extreme temperatures. *Structure* **3**, 1147-1158
 28. Henning, M., Darimont, B., Sterner, R., Kirschner, K., and Jansonius, J.N. (1995) 2.0 Å structure of indol-3-glycerol phosphate synthase from the hyperthermophile *Sulfolobus solfataricus*: possible determinants of protein stability. *Structure* **3**, 1295-1306
 29. Asada, K., Kanematsu, S., Okada, S., and Hayakawa, T. (1980) Phylogenetic distribution of three types of superoxide dismutase in organisms and in cell organelles in *Chemical and Biochemical Aspects of Superoxide and Superoxide Dismutase* (Bannister, J.V. and Hill, H.A.O., eds.) pp. 136-153, Elsevier Science, Amsterdam
 30. Gregory, E.M. and Dapper, C.H. (1983) Isolation of iron-containing superoxide dismutase from *Bacteroides fragilis*: reconstitution as a Mn-containing enzyme. *Arch. Biochem. Biophys.* **220**, 293-300
 31. Gregory, E.M. (1985) Characterization of the O₂-induced manganese-containing superoxide dismutase from *Bacteroides fragilis*. *Arch. Biochem. Biophys.* **238**, 83-89
 32. Hassan, H.M. and Fridovich, I. (1977) Enzymatic defenses against the toxicity of oxygen and of streptonigrin in *Escherichia coli*. *J. Bacteriol.* **129**, 1574-1583
 33. Hassan, H.M. and Fridovich, I. (1979) Intracellular production of superoxide radical and of hydrogen peroxide by redox active compounds. *Arch. Biochem. Biophys.* **196**, 385-395
 34. Holland, H.D. (1973) The oceans: A possible source of iron in iron-formations. *Economic Geol.* **68**, 1169-1172
 35. Egami, F. (1975) Origin and early evolution of transition element enzymes. *J. Biochem.* **77**, 1165-1169
 36. Rutz, J.M., Abdullah, T., Singh, S.P., Kalve, V.I., and Klebba, P.E. (1991) Evolution of the ferric enterobactin receptor in gram-negative bacteria. *J. Bacteriol.* **173**, 5964-5974
 37. Thompson, J.D., Higgins, D.G., and Gibson, T.J. (1994) CLUSTAL W: improving the sensitivity of progressive multiple sequence alignment through sequence weighting, position-specific gap penalties and weight matrix choice. *Nucleic Acids Res.* **22**, 4673-4680